Plant Science 345 (2024) 112135

Contents lists available at ScienceDirect

Plant Science

journal homepage: www.elsevier.com/locate/plantsci

Ultrastructure and development of the floral nectary from *Borago officinalis* L. and phytochemical changes in its secretion

Angelo Gismondi [a,1], Gabriele Di Marco [a,2], Lorena Canuti [a], Maria Maddalena Altamura [b,3], Antonella Canini [a,*,4]

[a] Dept. of Biology, University of Rome Tor Vergata, Via della Ricerca Scientifica 1, Rome 00133, Italy
[b] Dept. of Environmental Biology, University of Rome Sapienza, P.le A. Moro 5, Rome 00185, Italy

ARTICLE INFO

Keywords:
Borage
Starflower
Boraginaceae
Transmission electron microscopy
Plant secondary metabolites
Nectar
Granulocrine secretion

ABSTRACT

Although Boraginaceae have been classified as good sources of nectar for many insects, little is still known about their nectar and nectaries. Thus, in the present contribution, we investigated the nectar production dynamics and chemistry in *Borago officinalis* L. (borage or starflower), together with its potential interaction capacity with pollinators. A peak of nectar secretion (~5.1 μL per flower) was recorded at anthesis, to decrease linearly during the following 9 days. In addition, TEM and SEM analyses were performed to understand ultrastructure and morphological changes occurring in borage nectary before and after anthesis, but also after its secretory phase. Evidence suggested that nectar was transported by the apoplastic route (mainly from parenchyma to epidermis) and then released essentially by exocytotic processes, that is a granulocrine secretion. This theory was corroborated by monitoring the signal of complex polysaccharides and calcium, respectively, via Thiéry staining and ESI/EELS technique. After the secretory phase, nectary underwent degeneration, probably through autophagic events and/or senescence induction. Furthermore, nectar (Nec) and other flower structures (i.e., sepals, gynoecia with nectaries, and petals) from borage were characterized by spectrophotometry and HPLC-DAD, in terms of plant secondary metabolites, both at early (E-) and late (L-) phase from anthesis. The content of phytochemicals was quantified and discussed for all samples, highlighting potential biological roles of these compounds in the borage flower (e.g., antimicrobial, antioxidant, staining effects). Surprisingly, a high significant accumulation of flavonoids was registered in L-Nec, with respect to E-Nec, indicating that this phenomenon might be functional and able to hide molecular (e.g., defence against pathogens) and/or ecological (e.g., last call for pollinators) purposes. Indeed, it is known that these plant metabolites influence nectar palatability, encouraging the approach of specialist pollinators, deterring nectar robbers, and altering the behaviour of insects.

1. Introduction

Nectar is a sugary solution that, together with pollen, represents the main reward to pollinators (e.g., honeybees) and to protectors (e.g., ants) against herbivores, although it may also act as a lure for animal prey in carnivorous plants (González-Teuber and Heil, 2009; Torre, 2019). Thus, the biochemical profile of this substance changes in accordance with its own function, maturity stage, exogenous contamination, and environmental conditions (Bogo et al., 2021; Chalcoff et al., 2017), making the investigations on nectar composition a fundamental research field to understand plant-animal interactions. In this regard, Bogo et al. (2021) have also suggested that nectar features may affect floral visitors' behaviour and fidelity.

Nectar is essentially made up of carbohydrates, fatty acids, proteins, and plant secondary metabolites. Fructose, glucose, and sucrose are the most abundant sugars of this natural matrix, although several other

* Corresponding author.
E-mail addresses: gismondi@scienze.uniroma2.it (A. Gismondi), gabriele.di.marco@uniroma2.it (G. Di Marco), mariamaddalena.altamura@uniroma1.it (M.M. Altamura), canini@uniroma2.it (A. Canini).
[1] **ORCID:** 0000-0002-9257-9667
[2] **ORCID:** 0000-0002-1369-4895
[3] **ORCID:** 0000-0001-9848-6579
[4] **ORCID:** 0000-0003-1132-8899

https://doi.org/10.1016/j.plantsci.2024.112135
Received 16 April 2024; Accepted 23 May 2024
Available online 24 May 2024

monosaccharides (e.g., arabinose, mannose) and disaccharides (e.g., maltose, trehalose) have been registered in traces (Baker and Baker, 1983; Petanidou, 2005). Together with them, lipids represent an excellent energy source for pollinators (Nicolson and Thornburg, 2007), while the enzymes are principally involved in carbohydrate metabolism and in the maintenance of the nectar redox cycle, responsible for protecting gynoecium against microbial invasion (Nepi et al., 2012; Gismondi et al., 2018). Regarding phytochemicals, alkaloids, terpenoids, and phenolics have been detected (Baker, 1977; Raguso, 2004; Irwin and Adler, 2008). In particular, four functions have been hypothesized for them: i) antioxidant effect; ii) antibacterial activity; iii) determinant of taste (i.e., deterrent for non-pollinators and pleasant for pollinators); iv) visual cue for insects (due to their fluorescent properties) (Thorp et al., 1975; Hagler and Buchmann, 1993; Gismondi et al., 2018).

Nectar is produced and secreted through a finely regulated process by specialised multicellular glandular structures, the nectaries, which occur both on vegetative (extrafloral) and reproductive (floral) organs (Fahn, 1988). Overall, nectaries vary widely in ontogeny, morphology, and structure according to several factors, such as tissue localisation, composition of their secretions, plant species, maturity of the organism, ploidy level, water availability, etc. (Nepi et al., 1996; Petanidou et al., 2000; Fahn and Shimony, 2001; Pacini et al., 2003). Anatomically, nectaries are constituted by two main tissues, that is epidermis and parenchyma, although the latter can be subdivided in subnectary and nectary layer (Nepi, 2007). Subnectary parenchyma is the innermost tissue, containing vascular bundles and consisting of big cells rich in chloroplasts and with large vacuoles, loose cytoplasm, and wide intercellular spaces (Stpiczyńska et al., 2005; Nepi, 2007). By contrast, the nectary parenchyma is made up of some layers of small and thin-walled isodiametric cells characterized by a dense cytoplasm, several little vacuoles, and large nuclei (Fahn, 1988; Stpiczyńska et al., 2005). Here, the pre-nectar, mainly deriving from the phloem sap, is transformed into nectar, through enzymatic re-elaboration and re-absorption processes (Orona-Tamayo et al., 2013). However, nectar can also come from the primary starch accumulated into chloroplasts and directly produced *in loco* by photosynthesis, especially when it is required at night or in short time (Vassilyev and Koteyeva, 2004; Pacini and Nepi, 2007; Gaffal, 2012). Nectar can be moved and released by an eccrine secretion (that is the molecular transport of single carbohydrates across the cell membrane/wall by specific carriers) or via a granulocrine process (or rather the movement of a sugary solution into vesicles toward the extracellular compartment) or through an holocrine release (namely cell disintegration and release of its content) (Razem and Davis, 1999; Fahn, 2000). Moreover, the epidermal cells, generally polyhedric, small (about 6 μm), and with large vacuoles, can release nectar outside also by trichomes, pores, modified stomata, microchannels, cuticle breakage, or degeneration by programmed death (Pacini et al., 2003; Stpiczyńska et al., 2005; Wist and Davis, 2006; Nepi, 2007).

The present contribution aims at characterizing the ultrastructure of the floral nectaries from *Borago officinalis* L. (commonly known as borage or starflower), an herbaceous species belonging to the family of Boraginaceae, and the phytochemical profile of nectar and flower organs of this species, at early and late stages from anthesis. Indeed, to date, only Tacina (1972) has investigated by microscopy approach the nectary from borage, focusing the attention on the parenchyma tissue and giving less emphasis to the epidermal layers and the nectar release. In this context, although the genetic mechanisms underlying the development of flowers have been quite well clarified in the last decades (Jack, 2004; Theissen and Melzer, 2007; Zhang et al., 2012; Ó'Maoiléidigh et al., 2014), the maturation process of the nectar glands in synchrony with that of the sexual organs remains one of the flowers' best kept secrets. In addition, the phenomenon of the release of nectar at specific timings and the molecular relationship among secretory structures, pollinators, and plant secondary metabolites still require further elucidations.

2. Materials and methods

2.1. Plant material

The plant material was collected from specimens of *B. officinalis* identified in the Botanical Gardens of Rome Tor Vergata and taxonomically classified by Prof. Antonella Canini. Flowers positioned at the same node on plants of equal size and without symptoms of pathology were selected, to minimize any potential variation in nectar production. Hence, a total of 150 flowers were tagged and 125 of them also protected from flower visitors (using 60x60x90 cm cages covered by tulle, mesh size: 1 mm) during the whole sampling period, which occurred in April-June of 2008 and 2009. Some botanical vouchers were deposited in the herbarium of the Dept. of Biology of the University of Rome Tor Vergata (cod. 34299a-r).

Nectar was gathered daily by a Hamilton syringe (max. vol. 50 μL), without removing flowers, from floral anthesis for 9 days and immediately stored at -80 °C. For this activity, every day, flowers were sampled and then bagged again until the next sampling. Nectaries were sampled from other flowers about 24 hours before anthesis, during the anthesis but also at the end of the secretory phase. Nectar (i.e. Nec) and portions of the flower structure (i.e., gynoecia, Gyn; petals, Pet; sepals; Sep) were gently picked up, both at anthesis (early-stage, E-; time 0) and after 9 days from this event (late-stage, L-), to be instantly processed for the quantitation of the secondary metabolites.

2.2. Morphological study and calcium intracellular localisation

Plant material was observed under a stereomicroscope (Leica Zoom 2000), for a preliminary evaluation. Thus, flowers presenting tissue damages and/or alterations were excluded from the investigation.

Sample fixation occurred as described in Canini et al. (2001) and Canini et al. (2004), with some modifications. Briefly, early- and late-stage nectaries were fixed by 3% glutaraldehyde in phosphate buffer (PB; 0.2 M, pH 7.2) for 3 h at 4 °C and then by 1% osmium tetroxide in PB for 2 h at room temperature. After 3 washings in PB, samples were dehydrated by consecutive resuspensions (10 min each) in ethanol at different concentrations (25%, 50%, 75%, 95%, and 100%).

For Scanning Electron Microscopy (SEM) investigation, fixed samples were further dehydrated by applying the critical point drying process, using a Baltec CPD 030 apparatus, and coated with a 10 nm gold layer (Agar Automatic Sputter Coater B7341). The observation was performed by a Stereoscan Cambridge 440 Scanning Electron Microscope at 15 kV.

For Transmission Electron Microscopy (TEM) analysis, fixed samples were included in epoxy resin (Epon 812, Epoxy embedding medium; Sigma-Aldrich) through to the following steps: ethanol/propylene oxide (1:1, v/v) for 10 min; propylene oxide (two times, 20 min each); propylene oxide/resin (3:1, v/v) for 30 min; propylene oxide/resin (1:1, v/v) for 45 min; propylene oxide/resin (1:3, v/v) for 45 min; resin for 120 min. Finally, the polymerisation step was performed at 60 °C for 48 h. At this point, samples were sectioned by a ultramicrotome (Sorvall MT-5000 Ultra Microtome), positioned on 300-mesh copper or gold grids, and subjected to double staining by 2% uranyl acetate for 20 min and Reynolds lead citrate for 5 min in the dark (Daddow, 1983). In parallel, some sections were also exposed to Thièry reaction (Thièry, 1967) for detecting complex polysaccharides. This protocol consisted of: 1% periodic acid for 30 min; 1% thiosemicarbazide in 10% acetic acid for 2 h; three washings, 20 min each, with acetic acid (at 10%, 5%, and 1%, respectively); two washings in bidistilled water, 20 min each; 1% silver proteinate for 30 min; three rapid washings in bidistilled water; and drying at room temperature. All samples were observed by a Zeiss CEM 902 Transmission Electron Microscope at 80 kV. In addition, control and citric acid-treated ultrathin plant sections (obtained from samples prepared for TEM but without staining) were placed on 600-mesh copper grids and subjected to Electron Spectroscopic Imaging

(ESI) and Electron Energy Loss Spectra (EELS) analyses, for the localisation of intracellular calcium by CEM-902 Zeiss microscope (30000X magnification), according to the same method of Canini et al. (2001). Signals were acquired at ΔE=365 eV, that is immediately beyond the ionization edge (IE; ΔE=346–359 eV), and at the pre-ionization state (PIE; ΔE=315 eV), considered as background. Then, they were converted to images by a digital image analyser associated with an IBAS 2000 image processing system. To validate ESI data, EELS profiles were obtained by an electron detector able to compare spectral traces of signal intensity with energy loss values. Inelastically scattered electrons of defined energy losses were captured through a 20-eV energy window, obtaining high-contrast darkfield images at energy loss between 150 and 250 eV.

2.3. Extraction and quantitation of plant secondary metabolites

Petals (i.e., corolla), sepals (i.e., calix) and gynoecia (i.e., stigma, style, ovary, and ovules), the latter including nectaries, were ground with mortar and pestle in presence of liquid nitrogen. Thus, 50 mg of these plant materials or nectar were resuspended in acidified hydro-alcoholic solution (50% methanol in water with 0.8% hydrochloric acid, v/v) and left in agitation for 24 h at 37 °C. After centrifugation at 11.000 g for 15 min, the supernatant was collected, filtered (0.22 μm, Sartorius), and analysed.

Simple phenols were quantified by the Folin-Ciocalteu assay, following the protocol of De Rossi et al. (2021). Results, obtained using a calibration curve (0–100 mg L^{-1}; $R^2 = 0.984$) adequately prepared with pure gallic acid (Sigma-Aldrich), were expressed as mg of standard equivalents per g of fresh weight material (mg SE g^{-1} FW).

The concentration of flavonoids was estimated applying aluminium chloride colorimetric method, as specified in Di Marco et al. (2014). Data, extrapolated by a calibration curve (0–100 mg L^{-1}; $R^2 = 0.978$) prepared using adequate doses of pure quercetin (Sigma-Aldrich), were reported as mg of standard equivalents per g of fresh weight material (mg SE g^{-1} FW).

Total anthocyanins were measured by the spectrophotometric procedure of Giusti and Wrolstad (2001). In particular, the quantitation was indicated as mg of cyanidin equivalents per g of fresh weight material (mg SE g^{-1} FW).

A High-Pressure Liquid Chromatography system associated with an SPD-M20A Diode Array Detector (HPLC-DAD; Shimadzu, Japan) was employed to detect and quantify 13 specific secondary metabolites in the plant samples. The chromatographic analysis was carried out using a Phenomenex Gemini NX C18 (5 μm × 4.6 mm × 150 mm) column and imposing a flow rate at 0.95 mL/min. To investigate phenols and flavonoids, acidified water (with trichloroacetic acid at pH 2.5) and acetonitrile were used as buffer A and B, respectively. In this case, the elution gradient adopted during the run was: t0 min (A 85%, B 15%); t20 min (A 65%, B 35%); t28 min (A 20%, B 80%); t33 min (A 20%, B 80%). For the study of anthocyanins, buffer A and B consisted in 5% formic acid and acetonitrile, while the elution gradient was set as follows: t0 min (A 90%, B 10%); t20 min (A 80%, B 20%); t30 min (A 75%, B 25%); t40 min (A 60%, B 40%); t60 min (A 50%, B 50%). Chromatographic profiles were acquired at 280, 360, and 520 nm. Plant compounds were identified by comparing their retention times and absorbance spectra with those of relative pure standards (Sigma-Aldrich). The latter were analysed, at different concentrations, to create calibration curves necessary for the estimation of the micrograms of each metabolite per gram of fresh weight material (μg/g FW).

2.4. Statistics

Data represent means ± standard deviation (S.D.) of four independent measurements (biological replicates), each one analysed three times (technical replicates). Results were subjected to one-way analysis of variance (ANOVA) and the mean differences were compared by the post-hoc lowest standard deviations (LSD) test, using Excel software (p values: $^*p<0.05$; $^{**}p<0.01$; $^{***}p<0.001$).

3. Results and discussion

3.1. Nectar production in B. officinalis drastically decreases after 5 days from anthesis

B. officinalis (borage or starflower) is a wild plant species native to Europe, North America, and Asia Minor, whose ethnobotanical use, in culinary and medicinal terms, has been handed down for centuries (Ramezani et al., 2020). This herb has an important role in maintaining ecological equilibria as it is highly attractive for insects, representing a rich source of sugars and amino acids in the form of nectar and pollen (Descamps et al., 2018).

In borage, flowers present nutation and are characterized by a 5-parted calyx, a corolla composed of five ovate-lanceolate light blue/purple petals (rarely pink), a syncarpous gynoecium with a superior ovary, and anthers that form a cone around the style. They are grouped in terminal or axillary inflorescences that form large scorpioid cymes and whose bloom begins in Spring and continues throughout the Summer. Nectaries are located on the receptacle below the four-loculed ovary, forming a disk-like ring as expected in Boraginaceae (Kugler, 1970; Tacina, 1973; Pignatti, 1982; Weryszko-Chmielewska, 2003; Nocentini et al. 2012; Sastry et al. 2019), and their secretion, classified as sucrose-dominant (Descamps et al., 2021), is released after anthesis and accumulated in a reservoir delimited by the petals and the fused stamens (Stawiarz et al., 2000). Nevertheless, little is still known about the ultrastructure of the nectary and the content of secondary metabolites in the nectar of the starflower. Therefore, aim of the present research was to fill this gap, collecting scientific information. In fact, to date, the microscopy analysis of borage nectary has been carried out only by Tacina (1972), but the author here has mainly investigated the parenchyma layer of the gland, providing poor evidence about the exact mechanism of nectar release by the epidermal cells. Consequently, the present work represents a confirmation of the data reported in Tacina (1972) and examines in depth the nectary ultrastructure at post-secretion stage, together with nectar secretion modality in this species. Moreover, the study of the biochemical changes induced on borage nectar and flower organs during anthesis represents a peculiar further aspect treated in the present contribution.

First, the nectar produced in *B. officinalis* flowers was collected daily, to estimate the amount of sugary solution secreted by the annular nectary (Fig. 1A) between anthesis (time 0) and the 9th day after this phenomenon (Fig. 1B). This timing was chosen considering the work of Nocentini et al. (2012) performed on another Boraginaceae species, *Cerinthe major* L., whose anthesis lasts about one week and overlaps with stigmatic receptivity and anther dehiscence. According to our experiments, the general nectar production trend in the starflower appeared quite linear ($R^2 = 0.95$) and, in the whole selected timeframe, each flower was estimated to release a mean value of 2.59 μL of nectar per day. The maximum secretion (i.e., 5.1 μL per flower) was recorded on the day of anthesis (time 0), and then diminished continuously until the 9th day (i.e., 0.3 μL). Significant variations between consecutive days were found in the passages 3rd-4th, 4th-5th, and 7th-8th day, although the most substantial reduction was observed between the 3rd and the 5th day (-61.5%). The sampling became arduous after the 9th day, since the nectar volume was always lower than 0.1 μL. Our data seem to be in line with those reported by Descamps et al. (2021) (i.e., a maximum of 6.1 μL of nectar per flower), who have demonstrated that the quantity of nectar released by starflowers is strongly dependent on several environmental factors (e.g., temperature, water availability). Our data would suggest that flowers of *B. officinalis* are prolific nectar producers, with respect to those from other species of the same family known to release low amounts of this sugary solution, like *C. major* (3.25 μL in the first three days from anthesis) (Nocentini et al., 2012).

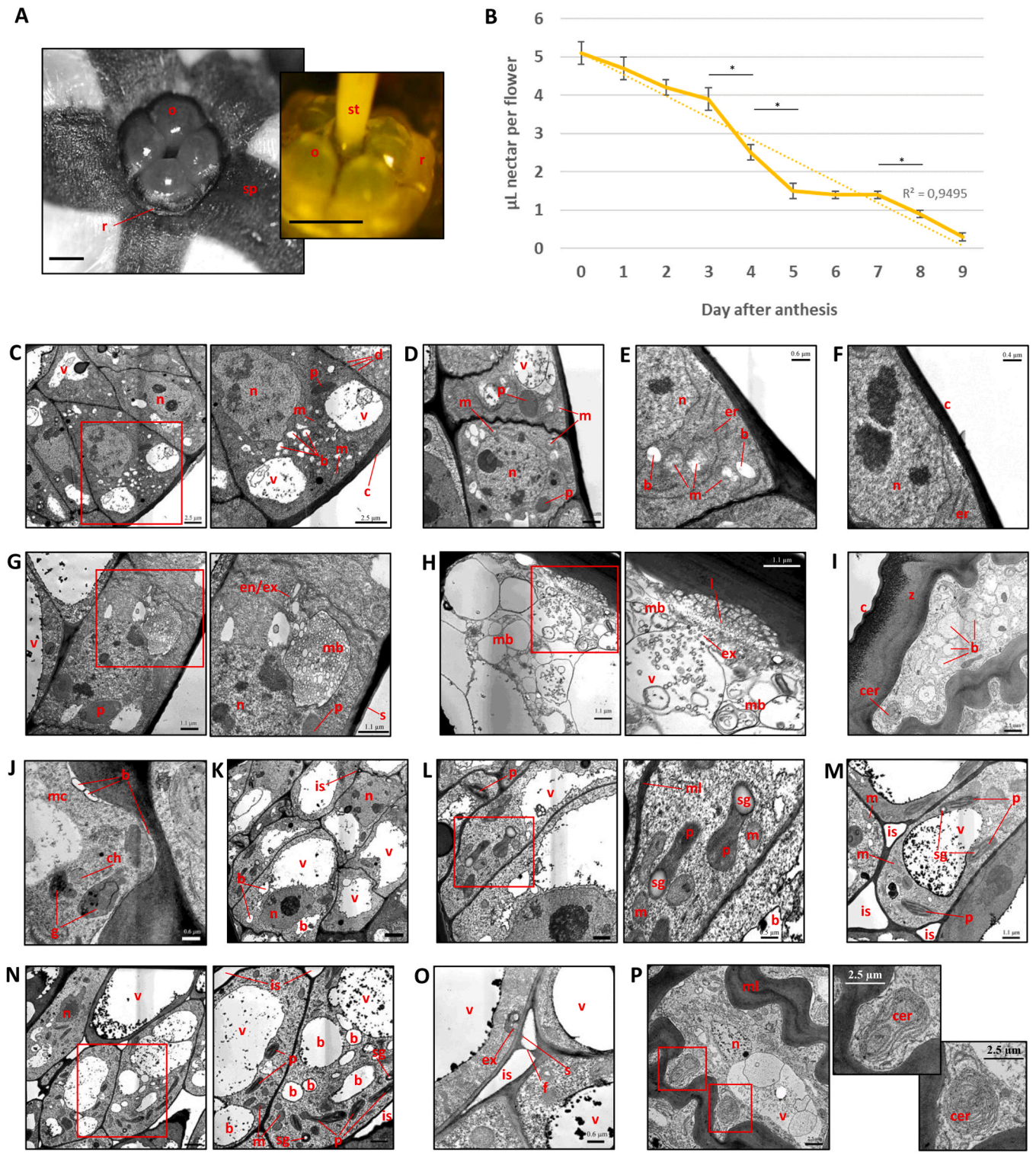

Fig. 1. Nectar yield and nectary ultrastructure. A) Stereomicroscopic images showing the ovaries and annular nectary per flower of *B. officinalis*. The black scale bars indicate 2 mm. **B)** Mean volume (± SD) of nectar secreted by borage flowers from anthesis (time 0) to the 9th day after this event. Significance was measured for each sampling day with respect to the following one (*$p<0.05$). **C-R)** Representative images of ultrathin sections from borage nectary captured by TEM (**C-J** and **K-P** images illustrate epidermal and parenchyma cells). The dimension bar is reported for each panel. In detail: **C)** epidermal layer at pre-anthesis stage (the right panel is the magnification of the red box in the left image); **D-H)** epidermal layer at post-anthesis (secretory) phase (in G and H, the right panels are the magnifications of the red boxes in the respective left images); **I-J)** epidermal layer at post-secretory stage; **K-L)** parenchymal layer at pre-anthesis stage (in L, the right panel is the magnification of the red box in the left image); **M-O)** parenchymal layer at post-anthesis (secretory) phase (in N, the right panel is the magnification of the red box in the left image); **P)** parenchymal layer at post-secretory stage (the right panels are magnifications of the red boxes in the left image). (Legend – b: vesicular body; c: cuticle; cer: concentric configurations of endoplasmic reticulum; ch: chromoplast; d: plasmodesmata; en: endocytotic event; er: endoplasmic reticulum; ex: exocytotic event; f: pectic filament; g: gerontoplast; is: intercellular space; l: lytic activity; m: mitochondrion; mb: multi-vesicular body; mc: membranous corpuscles; mL: middle lamella; n: nucleus; o- ovary; p: chloroplast; r: nectary lobe/ring; s: surface deposit; sg: starch granule; sp: sepal; st: style; v- vacuole; z: mineralization/lignification).

3.2. Ultrastructural modifications occur in borage nectary before and after the secretory phase

To investigate the ultrastructure of the borage nectary, a TEM analysis was performed. In particular, the plant tissue was collected before and after anthesis but also after the secretory phase, to elucidate the cytological changes induced by these two events on the nectary.

Overall, the nectary appeared composed by a single epidermal layer standing above parenchyma tissue. This evidence is in line with the literature, which documents that nectary epidermis normally exists in form of monolayer (Fahn, 1988).

Pre-anthesis epidermis (Fig. 1C) was made up of regular multifaceted cells showing medium-sized nuclei and vacuoles, sometimes flanked by smaller vacuolar structures. Moreover, they were rich in mitochondria and chloroplasts, occasionally containing small starch granules. The outer periclinal walls showed a thin cuticular layer, while the lateral ones were regular, quite thickened, and equipped with numerous plasmodesmata, whose detection has been also revealed by Tacina (1972). In numerous epidermal cells, a strong secretory activity, that is a cytoplasm full of exocytotic vesicles transporting their content towards the cell wall, was observed.

During post-anthesis, secretory stage (Fig. 1D-1 H), the epidermis was composed by polyhedral cells with thin and irregular lateral cell walls (Fig. 1D). Numerous mitochondria and plastids could be detected, the latter in a starch-free form (Figs. 1D and 1E). They also showed a large nucleus, rich in euchromatin, and a marked subcellular compartmentalization, mainly characterized by large vesicular bodies with probable secretory activity. Moreover, a surface deposit, probably nectar, could be highlighted above the cuticle. This evidence is not so unexpected, considering that in other species, like *Lamprocapnos spectabilis* (L.) Fukuhara (Papaveraceae), *Lonicera* sp. (Caprifoliaceae) and *Citrus* sp. (Rutaceae), nectar has been suggested to be exuded via microchannel or epidermis/cuticle pathway (i.e., permeable membranes) (Fahn, 1988; Landrein and Prenner, 2016; Zhang and Zhao, 2018). Indeed, interestingly, the cuticular layer on the apical cell walls tended to remain thin, like that found in pre-anthesis stage (Fig. 1F). In addition, in several cells, processes of endo- and exocytosis, ascribable to wide areas full of multi-vesicular bodies, were evident in the proximity of the radial and tangential cell walls, respectively (Fig. 1G). In particular, exocytotic phenomena were characterized by the release of lytic enzymes onto the tangential cell wall, in order to degrade it and allow nectar to be secreted (Fig. 1H).

After the secretory phase, the epidermis of the nectariferous tissue underwent an inactivation process, which included an extensive and irregular thickening of the radial and tangential cell walls with cuticle. In the same regions, secondary modification events (e.g., mineralization or lignification) could be detected (Fig. 1I). Vesicles and empty spaces were recorded both in the cytoplasm and between plasma membrane and cell wall, while numerous membranous corpuscles occurred only in the cytosol. Chloroplasts appeared converted into chromoplasts and gerontoplasts, nuclei contracted strongly, and the number of mitochondria reduced (Fig. 1J).

In parallel, the evolution of the parenchyma was monitored during the blossoming.

At pre-anthesis stage, the polyhedral cells of this tissue were generally compact; indeed, intercellular spaces could be visualized only rarely and in very small dimensions. The cells, delimited by evident primary walls and middle lamellae, were smaller than epidermal ones, similarly to those recorded in *L. spectabilis* (Zhang and Zhao, 2018). Moreover, they showed a reduced cytoplasm pushed against the plasmalemma and a large vacuole. Nuclei appeared rich in euchromatin, mitochondria were quite spherical, while chloroplasts presented bulky granules of primary starch. Accumulation of starch in pre-secretory stages has been associated with high levels of nectar production, representing the precursor of part of the sugars forming the nectar (Razem and Davis, 1999; Nepi, 2007). Indeed, in the case of low-nectar-producing plants, like in *C. major* (also a member of Boraginaceae), the pre-secretory parenchyma does not store starch, indicating that immediate photosynthesis represents the main source of nectar carbohydrates (Nocentini et al., 2012). Lastly, in borage parenchyma cells, some little vesicular structures, probably responsible for the accumulation of sugary substances deriving from phloem sap and to be transported towards the epidermis, were also detectable (Figs. 1K and 1L).

Post-anthesis parenchymal cells revealed shrunk nuclei, vacuoles reduced in size and often divided in sub-vesicles, but high density in mitochondria and chloroplasts. These plastids showed clearly distinguishable regular grana and still the capability to accumulate primary starch (Figs. 1M and 1N). Speaking of which, Wist and Davis (2006) have proposed that plastid starch granules, detectable in this and later phases, can sometimes represent the deposit of a nectar reabsorption process, preceding the cessation of the secretory activity. Large intercellular spaces existed in this tissue. There, it was possible to individuate: i) deposits on the cuticular surface, probably nectar; ii) exocytotic phenomena; iii) extracellular pectic filamentous structures. In particular, the latter seemed to connect adjacent cells for stabilizing the formation of secretion channels responsible for nectar transport (i.e., apoplastic route) (Fig. 1O).

Finally, in the post-secretory parenchyma, cells revealed a strongly thickened irregular cell wall, a degenerated nucleus, and, also in this case, evidence of organelle compartmentalization, especially at the expense of the ER which formed concentric configurations, already detected in Tacina (1972) as “corps lamellaires”. Moreover, mitochondria, chloroplasts and vesicular structures appeared progressively reduced and altered, suggesting an inactivation of the tissue (Fig. 1P).

Summarizing the collected evidence, we can state that borage nectary is made up of a specialized parenchyma, showing photosynthetic, temporary storage and transport functions, covered by an epidermal monolayer. During its development, this glandular tissue undergoes significant changes, moving from a condition of basal metabolic activity, typical of pre-anthesis phase, to a stage of hyperfunctionality, as suggested by the increase in chloroplasts and mitochondria recorded during the secretory phase. Here, chloroplasts, synthesizing glucose (and accumulating it in form of starch), would provide the sugary substance which constitutes the nectar, together with the phloem juice deriving by endocytosis from the underlying tissues (Castillo, 2016). Indeed, we did not observe complete vascular bundles within the secretory tissue, instead of other Boraginaceae species (Frei, 1955; Weryszko-Chmielewska, 2003). In this context, it is also fascinating to underline that in some Boraginaceae plants, such as *C. major*, an immediate photosynthesis would represent the main source of nectar carbohydrates, as we observed in borage (Nocentini et al., 2012). On the other hand, the high number of mitochondria would produce the force necessary to favour all the vesicular movements detected at this stage. Although a high energy demand has been generally linked to eccrine secretion (Razem and Davis, 1999), according to our evidence, borage nectary would release nectar by a granulocrine process. In support of this, we can mention that the number of vesicular bodies inside the cells increases in post-anthesis phase, in association to exocytotic processes aimed at releasing the nectar towards the outside, i.e. at the base of the gynoecium. The creation of intraparenchymal secretory channels and the occurrence of an intense intercellular vesicular traffic (also documented by irregularity, thinning, and degradation phenomena at the expense of the cell walls) would demonstrate that nectar is secreted in *B. officinalis* mainly through processes of reverse pinocytosis, a mechanism already proposed by Fahn (1988). However, it is not possible to exclude that nectar is released also via accessory structures, such as stomata (Dmitruk, 2019; Lustofin et al., 2020). Indeed, stomata have been detected on almost all floral nectaries from Boraginaceae (Hilger, 1985; Smets, 1986; Hilger, 1989), including *B. officinalis* (Caspary, 1848; Bonnier, 1879; Böhmker, 1917). On the other hand, it is extremely curious that in our microscopy observations such type of epidermal characteristics was not identified. In support of this, it is worthy of note

that also Tacina (1972) has not found stomata in their histological preparations from borage nectary. Thus, the most probable conclusion is that stomata are present in *B. officinalis* nectary, but probably shattered or obscured by debris during their microscopy preparations. In this regard, it is also important to underline that the system of nectar release is not always shared and conserved in all taxa of the same family; for instance, in *Myosotis sylvatica* Hoffm. (Boraginaceae) nectar is secreted by complex of aggregated stomata constantly open from anthesis (Weryszko-Chmielewska, 2003). Although all our data would indicate the apoplastic pathway as the election route for nectar translocation from parenchyma to epidermis, the existence of a simultaneous symplastic transport (i.e., by plasmodesmata) at the expense of nectary epidermal cells cannot be excluded. Indeed, in many species, it has been demonstrated that the combination of these two routes allows nectar transport and release (Wist and Davis, 2006). As regards the extracellular pectic filamentous structures found in our samples, they have already been described in chlorophyll and nectar-forming parenchymal tissues, playing important roles in storing reserve substances and conveying water (Machado et al., 2000; Paiva and Machado, 2008). Once the secretory phase has finished, nectaries are no longer necessary; therefore, both their epidermal and parenchymal cells are subjected to degeneration, as suggested by the generation of numerous cytoplasmic membranous corpuscles (maybe microautophagosomes?), wrinkling of the nuclei, conversion of chloroplasts into chromoplasts and gerontoplasts, and mineralization/lignification of the cell wall, or rather all events usually associated with programmed cell death and/or senescence (van Doorn and Woltering, 2004; Cutler and Somerville, 2005; van Doorn and Woltering, 2010; Bauer et al., 2011; Biswal et al., 2012; Zexer et al., 2023). In aid of this theory, we also observed the compartmentalization of cytoplasmic organelles, and particularly the formation of concentric configurations of ER, first described in potato by Shih and Rappaport (1971), whose function still unknown has been linked to a very low metabolic state, typical of degenerating cells (Rinne and Schoot, 2004). Several works have described the ER as a key organelle in granulocrine secretion, acting as producer of vesicles (Eriksson, 1977); therefore, the ER inactivation observed at post-secretory phase in starflower can be considered as an awaited phenomenon. In addition, the continuous enlargement of the vacuole and the presence of a high number of multivesicular bodies at this stage would corroborate the activation of autophagic events and the onset of senescence, as previously reported in *P. sativum* (Razem and Davis, 1999).

3.3. Calcium signal co-localises with the transfer of polysaccharides in the nectary tissue

Thiéry staining, able to mark complex polysaccharides, was performed on ultrathin sections of borage nectary and visualized by TEM analysis. The secretory epidermis showed numerous drops of polysaccharides mainly localised in the vacuoles and tending to exit from the tonoplast in vesicular bodies moving towards the cell wall (Fig. 2A-2 C). Indeed, as reported by Vesprini et al. (2008), the secretory material released by the nectary epidermis of *Helleborus foetidus* L. would be highly reactive to Thiéry staining. Worthy of note is the evidence that we collected about the parenchyma tissue of borage nectary where, at post-anthesis (secretory) stage, polysaccharides gathered in the intercellular spaces (Fig. 2D). The presence of complex carbohydrates in these channels for nectar transport, as well as in the cell wall region, has been documented also in some Cactaceae species (Silva et al., 2020), although its function remains unclear. Sawidis (1998) has suggested that these sugars may represent a mucilaginous matrix favouring the maintenance of the osmotic pressure and thus the apoplastic movement of the pre-nectar. However, other functional interpretations for this substance have been hypothesised, such as source of simple sugars and/or protection for the pre-nectar.

Calcium, together with hormones and oxygen and nitrogen reactive species, represents one of the main signalling molecules in the plant kingdom (Bowler and Fluhr, 2000; Sadak, 2016). This metal is involved in nearly all plant developmental processes, also triggering and modulating endocytosis and exocytosis phenomena. Thus, a finely regulated spatial and temporal control of Ca^{2+} concentrations is crucial for the correct functioning of plant cells and tissues (Chen et al., 2009; Batistič and Kudla, 2010; Vanneste and Friml, 2013). For this reason, we decided to localise calcium ions in ultrathin sections from starflower nectary. To obtain the best spatial resolution, the ESI/EELS technique was applied. A strong signal widely scattered in the cytoplasm could be detected in the epidermal cells at post-anthesis secretory phase (Fig. 2E). However, in some cases, the sensor clearly drew a concentration gradient, starting from the centre of the cell towards the cell wall (Fig. 2F). This mobilization of high quantities of intracellular calcium was perfectly consistent with the secretory activities previously hypothesized to the expense of the epidermal layer via exocytosis. On the other hand, in the parenchyma samples at the secretory stage, calcium ions mainly accumulated into the apoplastic region (i.e., cell wall and intercellular spaces), or rather where the pre-nectar is released and transported (Fig. 2G-2 H).

All these data would support further our previous hypothesis about the occurrence of a granulocrine process during the nectar release in starflower.

3.4. SEM analysis reveals the evolution of the epidermal layer in borage nectary

To obtain other information about the nectary glands from *B. officinalis*, a SEM analysis was carried out on plant material sampled at different blooming stages.

The microscopic characterization revealed for pre-anthesis nectary an epidermal surface made up of regular, ovoidal (about 9 ×6 μm), compressed, and convex cells lacking secretory structures, like trichomes or papillae, but homogenously covered by cuticle (Fig. 2I). At this phase, in fact, no secretion was released, and the epidermal layer needs to be compact.

During the secretory stage, both size and shape of the cells changed rapidly. Immediately after anthesis, the epidermal cells acquired a more irregular aspect, or rather they became polyhedral, non-uniform, and varied in dimensions (Fig. 2J). However, they still partially presented a convex nature, probably due to their content of sugars, used to form pre-nectar in due time (Chwil et al., 2019), which determine turgidity recalling water. Here, cutin arranged both on the cell surfaces but mainly, in form of narrow cuticular cords, in the periphery of the cells (Fig. 2K). By contrast, during the late phase of anthesis, the epidermal cells were flat, or even concave, strongly altered and sometimes broken. Indeed, the continuity of this superficial layer was often interrupted by micropores, quite probably the stomata suggested by the previous literature on *B. officinalis* (Caspary, 1848; Bonnier, 1879; Böhmker 1917), which should represent the way of release for nectar towards the outside. In support of this, it is interesting to observe the presence of sugary crystalline substances (i.e., the nectar carbohydrates) around and near the micropores (Fig. 2L-2 N). However, since some epidermal cells could be collapsed, taking into consideration their concavity and the activation of the cell death processes documented by our TEM analysis, it cannot be excluded that those micropores were also manifestations of degenerative cells. Indeed, in *Hexisea imbricata* (Lindl.) Rchb.f. (Orchidaceae), once nectar secretion is completed, some epidermal cells collapse, remaining compressed between the two tangential cell walls, while others remain intact and probably still functional (Stpiczyńska et al., 2005).

At the post-secretory step, nectary tended to degenerate. In particular, the epidermis of this gland showed features typical of the inactivation process for nectar secretion, that is an abundant deposition of cutin on its surface (Mačukanović-Jocić et al., 2007). In detail, long cutin fibers (whose thickness reached 2 μm) grouped together into overlapped bundles and tangential cracks could be detected only rarely

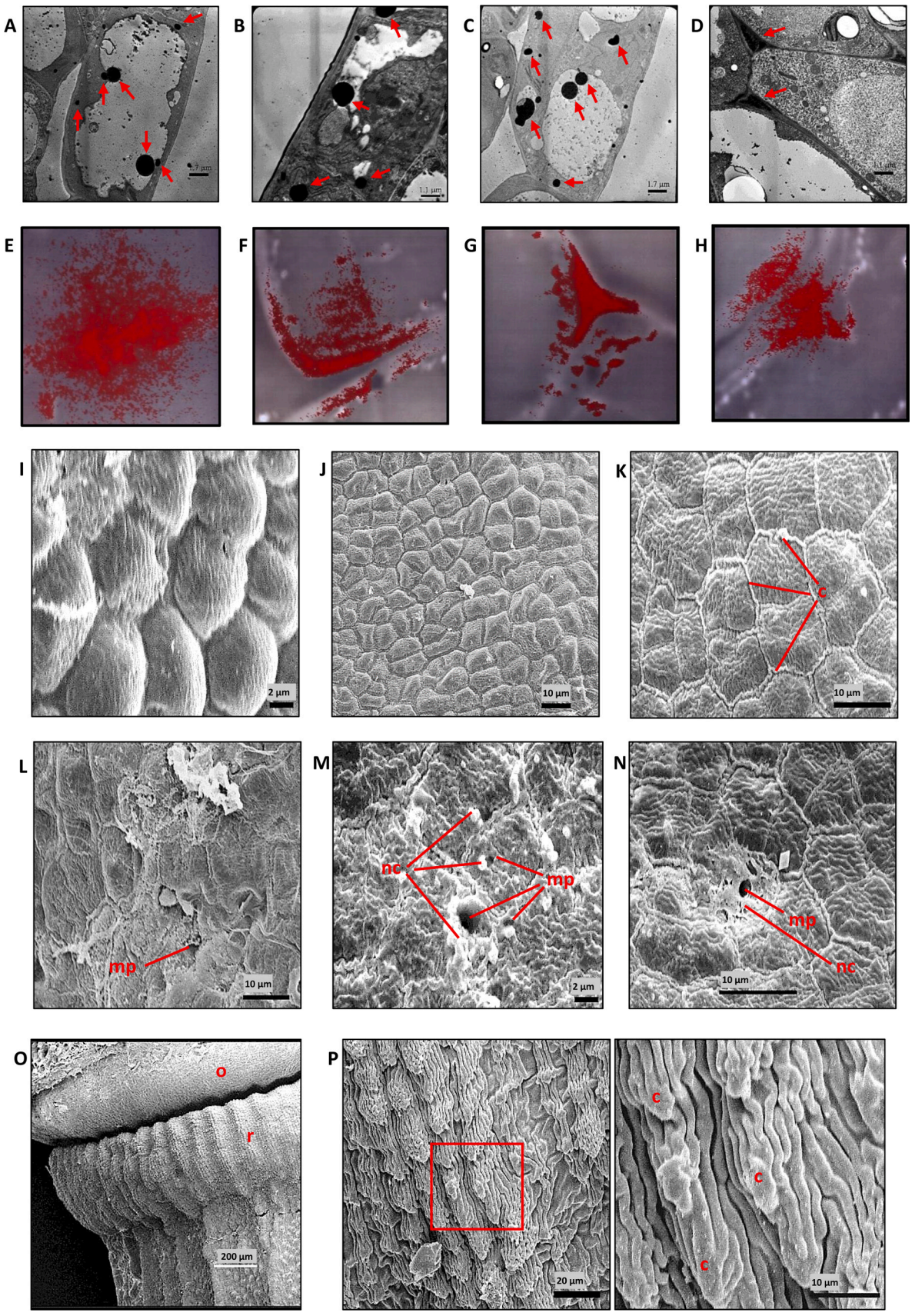

(caption on next page)

Fig. 2. Thiery staining, ESI/EELS and SEM analyses. A-D) Representative images of ultrathin sections from borage nectary captured by TEM after Thiery staining application. The dimension bar is reported for each panel. In detail: **A-C)** epidermal layer at post-anthesis (secretory) phase; **D)** parenchymal layer at post-anthesis (secretory) phase. Black spots (the biggest ones pointed out by red arrows) represent polysaccharide accumulations. **E-H)** Representative images of ultrathin sections of cells from borage nectary subjected to ESI and EELS analysis. In detail: **E-F)** cells and intercellular spaces from epidermal layer at post-anthesis (secretory) phase; **G-H)** intercellular spaces from parenchymal layer at post-anthesis (secretory) phase. The red signal represents calcium localisation. **I-P)** Representative images of borage nectary capture by SEM. The dimension bar is reported for each panel. In detail: **I)** epidermal layer at pre-anthesis phase; **J-N)** epidermal layer at post-anthesis phase (**J** and **K**: early secretory stage; **L, M** and **N**: late secretory stage); **O)** junction between nectary and ovary at post-secretory stage; **P)** epidermal layer at post-secretory stage (the right panel is the magnification of the red box in the left image). (Legend - c: cuticle; mp: micropore; nc: nectar carbohydrates; o- ovary; r: nectary lobe/ring).

(Figs. 2O and 2P). Although we suppose that the cuticular coating represented essentially an indicator of the nectary degeneration as usually linked to nectary ontogenesis but absent on the secretory districts (Mačukanović-Jocić et al., 2007; Stahl et al., 2012), the possibility that this substance (permeable to sugars) might represent an accumulation site of nectar residues even in the post-secretory phase should be considered, since in various orchid species this phenomenon has been recorded (Stpiczyńska, 2003; Stpiczyńska et al., 2004).

3.5. Borage nectar accumulates high levels of phenolics as flowering progresses

The last objective of this work was aimed at investigating the changes occurring at biochemical level, in terms of plant secondary metabolites, in the borage nectar (Nec), both at early (E-) and late (L-) stages from anthesis, with respect to those of other flower organs (i.e., sepals, Sep; gynoecia, Gyn; petals, Pet). At the beginning of our investigation, we decided to analyse the content of secondary metabolites both in nectaries and gynoecia. The preliminary analysis revealed that these two plant tissues presented very similar levels of phytochemicals, without any significant difference. Thus, taking into account this evidence and having noticed that it was very arduous to separate precisely ovaries from nectaries, we decided to collect gynoecium (that is stigma, style, ovary and ovules) and nectary glands together for the biochemical analyses.

Spectrophotometric analyses quantified the total content of simple phenols, flavonoids, and anthocyanins in the various samples (Fig. 3A).

Simple phenols ranged from 1.87 (in E-Nec) to 3.99 mg SE g^{-1} FW (in L-Pet). These phytochemicals showed a similar level in Nec and Sep samples, but were more concentrated in Gyn and Pet, probably due to their protective and vexillary role in these tissues (González-Teuber and Heil, 2009; Harborne and Grayer, 2017). Taking into consideration the two sampling stages (i.e., E- and L-), they changed significantly ($p<0.01$) only in the gynoecium, suggesting a key function of these compounds (which needs to be further investigated) during the final maturation steps of the female reproductive organs and/or the fertilisation event.

Overall, the content of flavonoids did not vary excessively in the whole series, starting from 1.30 mg SE g^{-1} FW in E-Nec and reaching 2.42 mg SE g^{-1} FW in E-Pet. Sepals and gynoecia were the poorest samples, together with E-Nec, while petals appeared the richest ones for these polyphenols. This evidence was quite expected, considering that flavonoids are the main plant pigments responsible for flower colouring (Harborne and Grayer, 2017). Indeed, the quantitation of the anthocyanins, a sub-class of flavonoids characterized by a typical purple-blue staining, revealed the presence of these substances exclusively in the petals, or rather the only flower portion presenting a violet shade. Interestingly, we observed that, compared to simple phenols, flavonoids increased ($p<0.01$) in L-Nec with respect to E-Nec. This result could be linked to a specific biological activity performed by the polyphenols in the late phases following anthesis; for example, they might be involved in the nectar redox cycle for their well-known antioxidant potential or antifungal and antibacterial properties able to limit the microbial growth (González-Teuber and Heil, 2009; Gismondi et al., 2018). On the other hand, the significant reduction ($p<0.01$) of the anthocyanins in L-Pet (*vs* E-Pet) would represent a consequence of the degeneration of the petals, which would start after nectar secretion phase when the attractive function of these flower organs is not required anymore.

Although the content of phenols and flavonoids in the nectar was equal or slightly lower than in the other samples, the level of these phytochemicals should be considered worthy of note, given that they come from a secretion and not a plant tissue. Moreover, our results would suggest that borage nectar is richer in secondary metabolites than others documented in the literature, such as *Robinia pseudoacacia* L. and *Allium cepa* L. (Soto et al., 2014; Gismondi et al., 2018).

Scientific data have demonstrated that insects are able to perceive secondary metabolites (e.g., phenolics, alkaloids) in plant tissues and secretions (Simmonds, 2001). In fact, beyond having antioxidant and antimicrobial properties, the existence of these compounds in the nectar would seem to carry out peculiar ecological functions, such as encouraging the approach of specialist pollinators, deterring nectar robbers, and altering the behaviour of insects. However, to date, it not clear if the accumulation of phytochemicals in the nectar is due to direct selection or to the simple consequence of their presence in phloem (Adler, 2000). Nevertheless, they are considered as key components of the nectar and, among them, the phenolics would influence particularly its aroma and attractive potential (Baker, 1977; Adler, 2000). For instance, Gong et al. (2021) have proved that solutions containing polyphenols increase memory retention and affect sensitivity to bee-alarm odours. According to all this premise, the final part of our study focused on the detection and quantitation of specific plant secondary metabolites in borage nectar and flower tissues. Indeed, although Boraginaceae have been classified as good sources of nectar for many insects, little is known about their nectar chemistry and interaction with pollinators (Nocentini et al., 2012).

HPLC-DAD approach (Fig. 3B-3E and Supplemental Material 1–4) allowed us to analyse the presence of 13 phenolic compounds, selected for their ubiquitous nature and peculiar bioactivity, in our samples (Table 1).

Overall, the levels of the investigated secondary metabolites appeared higher in the borage nectar than in those from other species, like acacia tree, onion, and sour cherry (Soto et al., 2014; Guffa et al., 2017; Gismondi et al., 2018), corroborating the previous spectrophotometric observation on total contents.

Caffeic acid, whose content ranged between 0.48 and 1.68 μg/g FW as the less concentrated among all the studied molecules. It did not vary significantly in the various samples between the E- and L- phases, except in nectar where this phenolic acid decreased with the progression of anthesis. This aspect could be justified considering that low concentrations of caffeic acid are preferred by pollinators, probably due to the repellent taste that this metabolite would provide to the nectar in high doses (Hagler and Buchmann, 1993). Thus, L-Nec would become less deterrent by reducing its level of caffeic acid, maybe to favour the call of insects even in the last stages of pollination. In this context, it is not possible to exclude that Caffeic acid, after its synthesis, was immediately converted in its derivatives (i.e., Chlorogenic acid and *p*-Coumaric acid), for limiting insects' repulsion towards *B. officinalis* flowers. In fact, the concentration of these last two phenolic acids was always higher than caffeic acid itself and showed a generally opposite accumulation trend between E- and L- experimental points.

All the flavonoids we measured (i.e., Kaempferol, Myricetin, Naringenin, Quercetin, and Apigenin) showed the same trend, or rather they highly accumulated in L-samples compared to the respective E-ones.

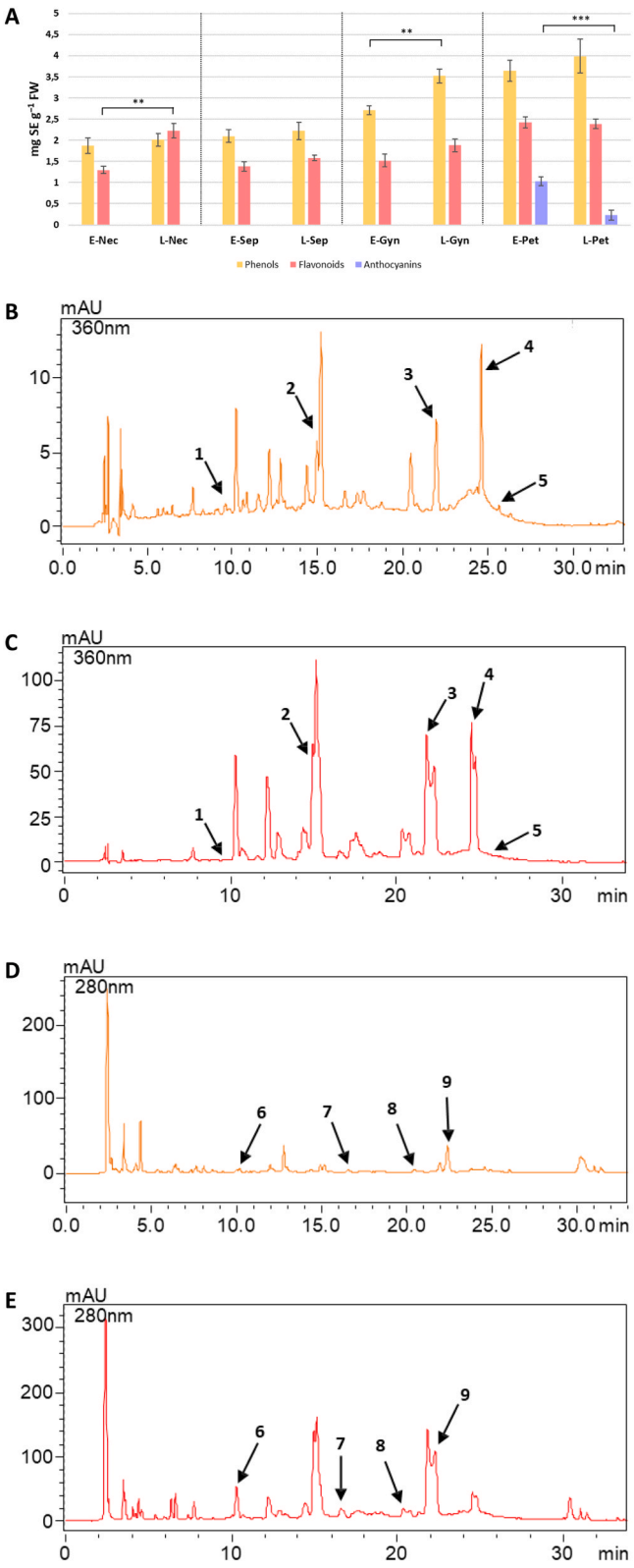

Fig. 3. Nectar biochemical profile. A) Spectrophotometric quantitation of total simple phenols, flavonoids, and anthocyanins in *B. officinalis* nectar (Nec), sepals (Sep), gynoecia (Gyn) and petals (Pet) sampled both at anthesis (early-stage, E-, time 0) and after 9 days from this event (late-stage, L-). Results are expressed as mg of standard equivalent per gram of plant fresh weight. The significance of the data was estimated, for each sample typology, between E- and L-stage (**$p<0.01$). **B-E)** Representative HPLC-DAD profiles for E-Nec (panels B and D) and L-Nec (panels C and E) were shown. On the x-axis is indicated the time (in minutes), whereas on the y-axis the milli-absorbance units (mAU) at 360 (panels B and C) or 280 nm (panels D and E) are reported. (Legend – 1: Caffeic acid; 2: Chlorogenic acid; 3: Kaempferol; 4: Myricetin; 5: Citropten; 6: *p*-Coumaric acid; 7: Naringenin; 8: Quercetin; 9: Apigenin).

Table 1
HPLC-DAD results. The chromatographic quantitation of specific plant secondary metabolites, with relative molecular classification and retention time (Rt), are reported as micrograms of standard equivalents per gram of fresh weight material (μg/g FW) for the investigated flower components. The significance of the data was estimated, for each sample typology, between E- (early) and L- (late) form (*$p<0.05$; **$p<0.01$; ***$p<0.001$). (Legend – Nec: nectar; Sep: sepals; Gyn: gynoecia; Pet: petals; n.d.: not detected).

Compound	Classification	Rt	E-Nec	L-Nec	E-Sep	L-Sep	E-Gyn	L-Gyn	E-Pet	L-Pet
Caffeic acid	Phenolic acid	*9.64*	1.50±0.07	0.96±0.06*	0.64±0.03	0.48±0.02	1.48±0.09	1.11±0.05	1.36±0.04	1.68±0.05
Chlorogenic acid	Phenolic acid	*14.99*	23.10 ±1.09	278.88 ±12.11***	55.23 ±3.04	72.54±4.05	21.11 ±1.02	38.17 ±2.09*	22.81±1.80	40.27±2.15*
Kaempferol	Flavonoid	*21.84*	27.09 ±1.88	265.12 ±14.25***	41.22 ±2.66	54.76±2.74	26.88 ±2.15	50.14 ±3.51*	26.98±2.01	34.68±2.64
Myricetin	Flavonoid	*24.66*	25.27 ±2.01	160.33±6.14***	8.42±0.98	12.63±0.75	29.47 ±1.11	46.31 ±2.01*	30.12±1.40	35.78±1.83
Citropten	Coumarin	*25.58*	4.53±0.23	2.73±0.08*	5.48±0.23	5.51±0.23	5.49±0.28	8.55±0.36*	3.66±0.19	12.22±0.55**
p-Coumaric acid	Phenolic acid	*10.32*	4.23±0.19	27.54±1.39***	8.58±0.56	11.10±0.69	4.57±0.21	8.23±0.32*	4.58±0.18	9.21±0.35**
Naringenin	Flavonoid	*16.5*	2.45±0.10	60.81±3.12***	2.72±0.15	2.63±0.19	2.54±0.16	2.81±0.12	2.39±0.10	31.42 ±1.51***
Quercetin	Flavonoid	*20.45*	28.33 ±1.65	85.12±4.36**	16.77 ±1.01	24.18 ±1.54*	24.22 ±1.78	40.35 ±2.88*	24.85±1.34	41.01±2.36*
Apigenin	Flavonoid	*22.50*	15.68 ±0.81	90.12±4.26***	14.86 ±0.79	18.16±1.01	28.07 ±2.10	51.19 ±2.36*	28.89±2.06	48.50±2.36*
Delphinidin	Anthocyanin	*14.85*	n.d.	n.d.	n.d.	n.d.	n.d.	n.d.	160.01 ±9.03	10.81 ±0.82***
Cyanidin	Anthocyanin	*16.18*	n.d.	n.d.	n.d.	n.d.	n.d.	n.d.	30.76±1.44	n.d.***
Peonidin	Anthocyanin	*28.01*	n.d.	n.d.	n.d.	n.d.	n.d.	n.d.	21.39±1.20	n.d.***
Malvidin	Anthocyanin	*30.03*	n.d.	n.d.	n.d.	n.d.	n.d.	n.d.	18.27±1.23	n.d.***

These increases were not so prominent in sepals, while in gynoecia ($p<0.05$), petals ($p<0.05$, for Naringenin $p<0.001$) and nectar ($p<0.001$, for Quercetin $p<0.01$) they were even very significant. In general, Kaempferol, Myricetin, and Quercetin were the most abundant polyphenols in the nectar; in petals, Apigenin stood out with the highest values, whereas in gynoecia and petals all flavonoids presented a similar content, except Naringenin.

The protective role of flavonoids in plants has been widely documented in the literature (Treutter, 2006). Consequently, the presence of these molecules in the nectar and in other flower tissues can be attributed to this basal defensive effect (e.g., in the gynoecium) or to their function as attractants (e.g., in petals); however, the extraordinary production of flavonoids we registered in the L-samples, especially Nec, might indicate the necessity to intensify the resistance against pathogens (e.g., bacteria, fungi, phytoviruses, viroids) and herbivores (e.g., in form of larvae) in the late steps of the blooming, when plant tissues undergo degeneration, senescence (e.g., petals), or structural changes (e.g., gynoecium), becoming, together with the nectar, fertile land for these colonisers involuntary transported by flower visitors or accidentally arrived there (Mallikarjuna et al., 2004; Ferrari et al., 2006).

A high ratio between Quercetin and Kaempferol has been correlated with photoprotective effects in *Petunia* Juss. leaves (Ryan et al., 2002); in our case, such type of datum was observed only in the sepals, as expected if one considers them like the simplest flower organs of the flower structure and so very similar to leaves, and in L-Nec. About the latter sample, the putative light shielding role would seem to be implausible, considering that in the late phase nectar has already carried out its function and has been exposed to the environment for several days.

Together with Quercetin, Naringenin has been recognized as a possible disincentive signal for honeybees, being able to reduce nectar palatability (Hernández et al., 2019). Maybe for this reason, it appeared as the least abundant among the quantified flavonoids both in E-Nec (2.45 μg/g FW) and in L-Nec (60.81 μg/g FW) samples. However, to date, its presence in nectar has not been fully understood.

Myricetin and Apigenin are, respectively, a flavanol and a flavone known for their antiradical properties but also for the capacity to induce the expression of antioxidant genes (Xie et al., 2013; Mekawy et al., 2018). In our context, since they increased in all L-samples, it is possible that these flavonoids worked as radical scavengers, to maintain the redox equilibrium in the aging flower tissues, including nectar.

Beyond the capacity to promote iron uptake, coumarins have been widely acknowledged as potential defence agents against infections (Stringlis et al., 2019). This biological role could justify the presence of Citropten in our samples of nectar, especially at the early stage (that is when the arrival of pollinators - and related microorganisms - is more frequent), and gynoecium, mainly at the late phase (that is when nectaries undergo deterioration and ovary is transformed into fruit). At the same time, surprisingly, the amount of this metabolite increased significantly ($p<0.01$) in L-Pet, reaching the maximum value of the series (12.22 μg/g FW). The explanation for this phenomenon remains difficult, considering that petals generally degenerate at the end of the blossoming and coumarins are weakly correlated with the antioxidant activity (Stringlis et al., 2019).

Taken all together, our data clearly showed that L-Nec presented the highest levels of all the phytochemicals we analysed in this study (especially flavonoids), except for Caffeic acid and Citropten. This evidence could suggest two main hypotheses: i) this accumulation of phenolics was functional and hid an ecological (e.g., last call for pollinators) and/or molecular (e.g., defence effect) purpose; ii) it depended on the fact that nectar was characterized by a lower content of water (or rather more concentrated) in the L-stage. However, the latter assumption would seem to be unlikely, since not all secondary metabolites accumulated in L-Nec compared to E-Nec (i.e., Caffeic acid and Citropten), suggesting that the biosynthesis of specific secondary metabolites (e.g., Chlorogenic acid, Kaempferol) occurred in L-Nec.

The last observation is related to the detection of anthocyanins (i.e., Delphinidin, Cyanidin, Peonidin, and Malvidin) only in petals, corroborating the previous spectrophotometric assay. These water-soluble pigments are mainly responsible for the colour of the borage corolla; indeed, as expected, they were present in high concentration in E-Pet, whereas only Delphinidin could be found in L-Pet samples, probably due to degradation process at the expense of these metabolites because of the beginning of flower degeneration.

Surely, it would be also interesting, in the future, to check if also an alkaloid fraction is present in borage flower tissues and nectar, as found in other Boraginaceae genera (e.g., *Echium*) (Lucchetti et al. 2016), since these phytochemicals (usually toxic) play other fundamental roles in modulating pollinator attraction.

4. Conclusions

In this work, production dynamics and chemistry of *B. officinalis*

nectar was investigated in detail, together with the ultrastructure of the flower nectary producing this sugary solution. We proved that starflower is one of the major producers of nectar in the family of Boraginaceae. In addition, the data we collected suggested the existence of a granulocrine secretion at the expense of this plant gland, which would undergo degeneration by authophagy or senescence at the end of its activity. Although borage nectar is full of phytochemicals, worthy of note is the fact that it increased the content of flavonoids after anthesis, maybe for defence purposes or to favour the last call for pollinators. Although further interesting studies could be carried out (for example, looking for microRNAs in the borage nectar and trying to understand if they can influence nectary development and secretion process), the present contribution defines the main features of the production system for borage nectar and reveals a potential key role of its chemical components in terms of interaction with pollinators.

CRediT authorship contribution statement

Angelo Gismondi: Conceptualization, Data curation, Supervision, Validation, Writing – original draft, Writing – review & editing. **Antonella Canini:** Conceptualization, Data curation, Resources, Validation, Writing – review & editing. **Lorena Canuti:** Investigation, Writing – review & editing. **Gabriele Di Marco:** Data curation, Investigation, Conceptualization, Writing – review & editing. **Maria Maddalena Altamura:** Conceptualization, Validation, Writing – review & editing.

Declaration of Competing Interest

The authors declare no conflict of interest about the present work.

Data Availability

All data are present in the paper are reported in the text or in the relative supplemental materials

Acknowledgment

None to declare.

Appendix A. Supporting information

Supplementary data associated with this article can be found in the online version at doi:10.1016/j.plantsci.2024.112135.

References

L.S. Adler, The ecological significance of toxic nectar, Oikos 91 (3) (2000) 409–420.

H.G. Baker, I. Baker, Floral nectar constituents in relation to pollinator type, in: C. E. Jones, R.J. Little (Eds.), Handbook of experimental pollination biology, Van Nostrand Reinhold, New York, NY, 1983, pp. 117–141.

H.G. Baker, Non-sugar chemical constituents of nectar, Apidologie 8 (1977) 349–356.

O. Batistič, J. Kudla, Calcium: not just another ion, in: R. Hell, R.R. Mendel (Eds.), Cell Biology of Metals and Nutrients. Plant Cell Monographs, vol 17, Springer, Berlin, Heidelberg, 2010.

P. Bauer, R. Elbaum, I.M. Weiss, Calcium and silicon mineralization in land plants: transport, structure and function, Plant Sci. 180 (6) (2011) 746–756.

B. Biswal, P.K. Mohapatra, U.C. Biswal, M.K. Raval, Leaf senescence and transformation of chloroplasts to gerontoplasts. In: Photosynthesis: plastid biology, energy conversion and carbon assimilation, Springer, 2012, pp. 217–230.

G. Bogo, A. Fisogni, J. Rabassa-Juvanteny, L. Bortolotti, M. Nepi, M. Guarnieri, M. Galloni, Nectar chemistry is not only a plant's affair: floral visitors affect nectar sugar and amino acid composition, Oikos 130 (7) (2021) 1180–1192.

H. Bohmker, Beitrage zur Kenntnis der floralen und extrafloralen Nektarien, Beih. Bot. Zent. 33 (1917) 169–247.

G. Bonnier, Les nectaries. Etude critique, anatomique et physiologique, Ann. Des. Sci. Nat. Bot. 8 (1879) 5–212.

C. Bowler, R. Fluhr, The role of calcium and activated oxygens as signals for controlling cross-tolerance, Trends Plant Sci. 5 (6) (2000) 241–246.

A. Canini, J. Giovinazzi, P. Iacovacci, C. Pini, M. Grilli Caiola, Localization of a carbohydrate epitope recognised by human IgE in pollen of Cupressaceae. J. Plant Res. 117 (2004) 147–153.

A. Canini, D. Leonardi, M. Grilli Caiola, S. Ruggeri, E. Carnovale, Intracellular localization of calcium, phosphorus and nitrogen in common bean seeds (*Phaseolus vulgaris* L. cv. Borlotto) by SEM, ESI and EELS techniques, Plant Biosyst. 135 (2) (2001) 123–132.

Caspary, I.X.R. (1848). De nectariis. Dissertation. J. Schellhoff – Elverfeldae (Bonn), pp 56.

Castillo, N.R.F. (2016). Carbohydrate composition and structure changes as phloem sap is converted to Nectar in *Borago officinalis* L. and select *Brassica* spp. L (Doctoral dissertation, University of Saskatchewan).

V.R. Chalcoff, G. Gleiser, C. Ezcurra, M.A. Aizen, Pollinator type and secondarily climate are related to nectar sugar composition across the angiosperms, Evolut. Ecol. 31 (4) (2017) 585–602.

T. Chen, X. Wu, Y. Chen, X. Li, M. Huang, M. Zheng, J. Lin, Combined proteomic and cytological analysis of Ca2+-calmodulin regulation in *Picea meyeri* pollen tube growth, Plant Physiol. 149 (2) (2009) 1111–1126.

M. Chwil, M. Kostryco, R. Matraszek-Gawron, Comparative studies on structure of the floral nectaries and the abundance of nectar production of *Prunus laurocerasus* L, Protoplasma 256 (2019) 1705–1726.

S.R. Cutler, C.R. Somerville, Imaging plant cell death: GFP-Nit1 aggregation marks an early step of wound and herbicide induced cell death, BMC Plant Biol. 5 (2005) 1–15.

L.Y.M. Daddow, A double lead stain method for enhancing contrast of ultrathin sections in electron microscopy: a modified multiple staining technique, J. Microsc. 129 (2) (1983) 147–153.

S. De Rossi, G. Di Marco, L. Bruno, A. Gismondi, A. Canini, Investigating the drought and salinity effect on the redox components of *Sulla coronaria* (L.) Medik, Antioxidants 10 (07) (2021) 1048.

C. Descamps, M. Quinet, A.L. Jacquemart, Climate change–induced stress reduce quantity and alter composition of nectar and pollen from a bee-pollinated species (*Borago officinalis*, Boraginaceae), Front. Plant Sci. 12 (2021) 755843.

C. Descamps, M. Quinet, A. Baijot, A.L. Jacquemart, Temperature and water stress affect plant–pollinator interactions in *Borago officinalis* (Boraginaceae), Ecol. Evol. 8 (6) (2018) 3443–3456.

G. Di Marco, A. Gismondi, L. Canuti, M. Scimeca, A. Volpe, A. Canini, Tetracycline accumulates in *Iberis sempervirens* L. through apoplastic transport inducing oxidative stress and growth inhibition, Plant Biol. 16 (4) (2014) 792–800.

M. Dmitruk, Flowering, nectar secretion, and structure of the nectary in the flowers of *Acer pseudoplatanus* L, Acta Agrobot. 72 (3) (2019).

M. Eriksson, The ultrastructure of the nectary of red clover (*Trifolium pratense*), J. Apic. Res. 16 (4) (1977) 184–193.

A. Fahn, Secretory tissues in vascular plants, N. Phytol. 108 (1988) 229–257.

A. Fahn, C. Shimony, Nectary structure and ultrastructure of unisexual flowers of *Ecballium elaterium* (L.) A. Rich. (Cucurbitaceae) and their presumptive pollinators, Ann. Bot. 87 (1) (2001) 27–33.

M. Ferrari, O. Bjornstad, J. Partain, J. Antonovics, A gravity model for the spread of a pollinator-borne plant pathogen, Am. Nat. 168 (2006) 294–303.

E. Frei, Die Innervierung der floralen Nektarien dikotyler Pflanzenfamilien, Ber. der Schweiz. Bot. Ges. 65 (1955) 60–114.

K.P. Gaffal, How common is the ability of extrafloral nectaries to produce nectar droplets, to secrete nectar during the night and to store starch? Plant Biol. 14 (5) (2012) 691–695.

A. Gismondi, S. De Rossi, L. Canuti, S. Novelli, G. Di Marco, L. Fattorini, A. Canini, From *Robinia pseudoacacia* L. nectar to Acacia monofloral honey: Biochemical changes and variation of biological properties, J. Sci. Food Agric. 98 (11) (2018) 4312–4322.

M.M. Giusti, R.E. Wrolstad, Characterization and measurement of anthocyanins by UV-visible spectroscopy. Curr. Protoc. Food Anal. Chem. (1) (2001) F1–F2.

Z. Gong, G. Gu, Y. Wang, S. Dong, K. Tan, J.C. Nieh, Floral tea polyphenols can improve honey bee memory retention and olfactory sensitivity, J. Insect Physiol. 128 (2021) 104177.

M. González-Teuber, M. Heil, Nectar chemistry is tailored for both attraction of mutualists and protection from exploiters, Plant Signal. Behav. 4 (2009) 809–813.

B. Guffa, N.M. Nedić, D.Ć. Dabić Zagorac, T.B. Tosti, U.M. Gašić, M.M. Natić, M. M. Fotirić Akšić, Characterization of sugar and polyphenolic diversity in floral nectar of different 'Oblačinska'sour cherry clones, Chem. Biodivers. 14 (9) (2017) e1700061.

J.R. Hagler, S.L. Buchmann, Honey bee (Hymenoptera: Apidae) foraging responses to phenolic-rich nectars, J. Kans. Èntomol. Soc. (1993) 223–230.

J.B. Harborne, R.J. Grayer, Flavonoids and insects, in: In the flavonoids advances in research since, 1986, Routledge, 2017, pp. 589–618.

I.G. Hernández, F. Palottini, I. Macri, C.R. Galmarini, W.M. Farina, Appetitive behavior of the honey bee *Apis mellifera* in response to phenolic compounds naturally found in nectars, J. Exp. Biol. 222 (2) (2019) jeb189910.

H.H. Hilger, Ontogenie, morphologie und systematische bedeutung geflügelter und glochiidientragender Cynoglossae- und Eritracheae-Früchte (Boraginaceae), Bot. Jahrb. fur Syst., Pflanzengesch. und Pflanzengeogr. 105 (3) (1985) 323–378.

H.H. Hilger, Flower and fruit development in the Macaronesian endemic *Ceballosia fruticosa* (syn. *Messerschmidia fruticose*, Boraginaceae, Helotropioideae), Bot. Jahrb. fur Syst., Pflanzengesch. und Pflanzengeogr. 105 (3) (1989) 323–378.

R.E. Irwin, L.S. Adler, Nectar secondary compounds affect self-pollen transfer: implications for female and male reproduction. Ecology 89 (8) (2008) 2207–2217.

T. Jack, Molecular and genetic mechanisms of floral control, Plant Cell 16 (suppl_1) (2004) S1–S17.

Kugler H., 1970 - Blütenökologie. G. Fischer Verlag, Stuttgart (eds.).

S. Landrein, G. Prenner, Structure, ultrastructure and evolution of floral nectaries in the twinflower tribe Linnaeeae and related taxa (Caprifoliaceae), Bot. J. Linn. Soc. 181 (1) (2016) 37–69.

M.A. Lucchetti, G. Glauser, V. Kilchenmann, A. Dubecke, G. Beckh, C. Praz, C. Kast, Pyrrolizidine alkaloids from *Echium vulgare* in honey originate primarily from floral nectar, J. Agric. Food Chem. 64 (25) (2016) 5267–5273.
K. Lustofin, P. Świątek, V.F. Miranda, B.J. Płachno, Flower nectar trichome structure of carnivorous plants from the genus butterworts *Pinguicula* L. (Lentibulariaceae), Protoplasma 257 (2020) 245–259.
S.R. Machado, M.E.M. Estelita, E.A. Gregório, Ultrastructure of the intercellular protuberances in leaves of *Paepalanthus superbus* Ruhl. (Eriocaulaceae), Rev. Bras. Bot. 23 (2000) 449–455.
M.P. Mačukanović-Jocić, D.V. Rančić, Z.D. Stevanović, Floral nectaries of basil (*Ocimum basilicum*): Morphology, anatomy and possible mode of secretion, South Afr. J. Bot. 73 (4) (2007) 636–641.
N. Mallikarjuna, K.R. Kranthi, D.R. Jadhav, S. Kranthi, S. Chandra, Influence of foliar chemical compounds on the development of *Spodoptera litura* (Fab.) in interspecific derivatives of groundnut, J. Appl. Entomol. 128 (2004) 321–328.
A.M.M. Mekawy, M.N. Abdelaziz, A. Ueda, Apigenin pretreatment enhances growth and salinity tolerance of rice seedlings, Plant Physiol. Biochem. 130 (2018) 94–104.
M. Nepi, F. Ciampolini, E. Pacini, Development and ultrastructure of *Cucurbita pepo* nectaries of male flowers, Ann. Bot. 81 (1996) 251–262.
M. Nepi, Nectary structure and ultrastructure, in: S.W. Nicolson, M. Nepi, E. Pacini (Eds.), Nectaries and Nectar, Springer, Dordrecht, 2007, pp. 129–166.
M. Nepi, C. Soligo, D. Nocentini, M. Abate, M. Guarnieri, C. Giampiero, L. Bini, M. Puglia, L. Bianchi, E. Pacini, Amino acids and protein profile in floral nectar: much more than a simple reward, Flora 207 (2012) 475–481.
S.W. Nicolson, R.W. Thornburg, Nectar chemistry, in: S.W. Nicolson, M. Nepi, E. Pacini (Eds.), Nectaries and Nectar, Springer, Dordrecht, 2007, pp. 215–264.
D. Nocentini, E. Pacini, M. Guarnieri, M. Nepi, Flower morphology, nectar traits and pollinators of *Cerinthe major* (Boraginaceae-Lithospermeae), Flora 207 (3) (2012) 186–196.
D.S. Ó'Maoiléidigh, E. Graciet, F. Wellmer, Gene networks controlling *Arabidopsis thaliana* flower development, N. Phytol. 201 (1) (2014) 16–30.
D. Orona-Tamayo, N. Wielsch, M. Escalante-Pérez, A. Svatos, J. Molina-Torres, A. Muck, M. Heil, Short-term proteomic dynamics reveal metabolic factory for active extrafloral nectar secretion by *Acacia cornigera* ant-plants. Plant J. 73 (4) (2013) 546–554.
E. Pacini, M. Nepi, Nectar production and presentation, in: S. Nicolson, M. Nepi, E. Pacini (Eds.), In: Nectaries and nectar, Dordrecht: Springer, 2007, pp. 167–214.
E. Pacini, M. Nepi, J.L. Vesprini, Nectar biodiversity: a short review, Plant Syst. Evol. 238 (2003) 7–21.
E.A.S. Paiva, R.S. Machado, Intercellular pectic protuberances in *Hymenaea stigonocarpa* (Fabaceae, Caesalpinioideae): Occurrence and functional aspects, C. R. Biol. 331 (2008) 287–293.
T. Petanidou, V. Goethals, E. Smets, Nectary structure of Labiatae in relation to their nectar secretion and characteristics in a Mediterranean shrub community – Does flowering time matter? Plant Syst. Evol. 225 (2000) 103–118.
T. Petanidou, Sugars in Mediterranean floral nectars: an ecological and evolutionary approach, J. Chem. Ecol. 31 (5) (2005) 1065–1088.
Pignatti S., 1982 - Flora d'Italia. Edagricole (eds.).
R.A. Raguso, Why are some floral nectars scented? Ecology 85 (6) (2004) 1486–1494.
M. Ramezani, M.S. Amiri, E. Zibaee, Z. Boghrati, Z. Ayati, A. Sahebkar, S.A. Emami, A review on the phytochemistry, ethnobotanical uses and pharmacology of *Borago* species, Curr. Pharm. Des. 26 (1) (2020) 110–128.
F.A. Razem, A.R. Davis, Anatomical and ultrastructural changes of the floral nectary of *Pisum sativum* L. during flower development, Protoplasma 206 (1999) 57–72.
P.L. Rinne, C.V.D. Schoot, Cell-cell communication as a key factor in dormancy cycling, J. Crop Improv. 10 (1-2) (2004) 113–156.
K.G. Ryan, E.E. Swinny, K.R. Markham, C. Winefield, Flavonoid gene expression and UV photoprotection in transgenic and mutant *Petunia* leaves, Phytochemistry 59 (1) (2002) 23–32.
M.S. Sadak, Physiological role of signal molecules in improving plant tolerance under abiotic stress, Int. J. ChemTech Res. 9 (7) (2016) 46–60.
K.S. Sastry, B. Mandal, J. Hammond, S.W. Scott, R.W. Briddon, K.S. Sastry, R.W. Briddon, *Borago officinalis* (Borage, Starflower), Encycl. Plant Virus Viroids (2019) 286.
T. Sawidis, The subglandular tissue of *Hibiscus rosa-sinensis* nectaries, Flora 193 (3) (1998) 327–335.
C.Y. Shih, L.R. Rappaport, Regulation of bud rest in tubers of potato, *Solanum tuberosum* L. VIII. Early effects of gibberellin A3 and abscisic acid on ultrastructure, Plant Physiol. 48 (1971) 31–35.
S.C.D.M. Silva, S.R. Machado, M. Nepi, T.M. Rodrigues, Structure and function of secretory glochids and nectar composition in two Opuntioideae (Cactaceae) species, Botany 98 (8) (2020) 425–437.
M.S.J. Simmonds, Importance of flavonoids in insect–plant interactions: feeding and oviposition, Phytochemistry 56 (2001) 245–252.
E. Smets, Localization and systematic importance of the floral nectaries in the Magnoliatae (Dicotyledons), Bull. du Jard. Bot. Natl. De. Belg. /Bull. Van. De. Natl. Plantentuin Van. Belg. 56 (1986) 51–76.
V.C. Soto, F.M. de los Ángeles, R. Galmarini C, S.M. Fernanda, Analysis of phenolic compounds in onion nectar by miniaturized off-line solid phase extraction-capillary zone electrophoresis, Anal. Methods 6 (13) (2014) 4878–4884.
J.M. Stahl, M. Nepi, L. Galetto, E. Guimarães, S.R. Machado, Functional aspects of floral nectar secretion of *Ananas ananassoides*, an ornithophilous bromeliad from the Brazilian savanna, Ann. Bot. 109 (7) (2012) 1243–1252.
E. Stawiarz, A. Wroblewska, M. Masierowska, D. Sadowska, Flowering, forage value, and insect pollination in *Borago* (L.) cultivated in Se Poland, J. Apic. Sci. 64 (1) (2000) 77–89.
M. Stpiczynska, K.L. Davies, A. Gregg, Nectary structure and nectar secretion in *Maxillaria coccinea* (Jacq.) L.O. Williams ex Hodge (Orchidaceae), Ann. Bot. 93 (2004) 87–95.
M. Stpiczynska, Nectar resorption in the spur of *Platanthera chlorantha* (Custer) Rchb. (Orchidaceae)—structural and microautoradiographic study, Plant Syst. Evol. 238 (2003) 119–126.
M. Stpiczyńska, K.L. Davies, A. Gregg, Comparative account of nectary structure in *Hexisea imbricata* (Lindl.) Rchb. f. (Orchidaceae), Ann. Bot. 95 (5) (2005) 749–756.
I.A. Stringlis, R. De Jonge, C.M. Pieterse, The age of coumarins in plant–microbe interactions, Plant Cell Physiol. 60 (7) (2019) 1405–1419.
F. Tacina, Ultrastructure of nectariferous cells in *Borago officinalis*, Rev. Roum. De. Biol., Bot. 17 (4) (1972) 227–234.
F. Tacina, La structure optique et électronmicroscopique de la glande nectarifère chez *Cynoglossum officinalis* L, Rev. Roum. De. Biol., Bot. 18 (1973) 201–209.
G. Theissen, R. Melzer, Molecular mechanisms underlying origin and diversification of the angiosperm flower, Ann. Bot. 100 (3) (2007) 603–619.
J.P. Thièry, Mise en evidence des polysaccharides sur coupes en microscopie electronique, Journ. Microsc. 6 (1967) 987–1018.
R.W. Thorp, D.L. Briggs, J.R. Estes, E.H. Erickson, Nectar fluorescence under ultraviolet irradiation, Science 189 (1975) 476–478.
Dan Torre, Carnivorous plants, Reaktion Books, 2019.
D. Treutter, Significance of flavonoids in plant resistance: a review, Environ. Chem. Lett. 4 (3) (2006) 147–157.
W.G. van Doorn, E.J. Woltering, Senescence and programmed cell death: substance or semantics? J. Exp. Bot. 55 (406) (2004) 2147–2153.
W.G. van Doorn, E.J. Woltering, What about the role of autophagy in PCD? Trends Plant Sci. 15 (7) (2010) 361–362.
S. Vanneste, J. Friml, Calcium: the missing link in auxin action, Plants 2 (4) (2013) 650–675.
A.E. Vassilyev, N.K. Koteyeva, Comparative analysis of vascular system structure in nectaries and minor leaf veins. 1. "Apoplasmic" species, Bot. Zh. . (St. Petersburg) 89 (2004) 1537–1553.
J.L. Vesprini, M. Nepi, F. Ciampolini, E. Pacini, Holocrine secretion and cytoplasmic content of *Helleborus foetidus* L. (Ranunculaceae) nectar, Plant Biol. 10 (2) (2008) 268–271.
E. Weryszko-Chmielewska, Morphology and anatomy of floral nectary and corolla outgrowths of *Myosotis sylvatica* Hoffm. (Boraginaceae), Acta Biol. Crac. Ser. Bot. 45 (1) (2003) 43–48.
T.J. Wist, A.R. Davis, Floral nectar production and nectar anatomy and ultrastructure of *Echinacea purpurea* (Asteraceae), Ann. Bot. 97 (2006) 177–193.
H.J. Xie, W.S. Mou, F.R. Lin, J.H. Xu, Q.F. Lei, Radical scavenging activity of myricetin, Acta Phys. -Chim. Sin. 29 (7) (2013) 1421–1432.
N. Zexer, S. Kumar, R. Elbaum, Silica deposition in plants: Scaffolding the mineralization, Ann. Bot. (2023) mcad056.
W. Zhang, E.M. Kramer, C.C. Davis, Similar genetic mechanisms underlie the parallel evolution of floral phenotypes, PLoS One 7 (4) (2012) e36033.
X. Zhang, L. Zhao, Morphology, structure and ultrastructure of staminal nectary in *Lamprocapnos* (Fumarioideae, Papaveraceae), Flora 242 (2018) 128–136.